Computational fluid dynamics modeling and hemolysis analysis of axial blood pumps with various impeller structures*

XIA Dongdong[1], ZHAO Chunzhang[2], ZHANG Xiwen[2] and BAI Jing[1]**

(1. Department of Biomedical Engineering, Tsinghua University, Beijing 100084, China; 2. Department of Engineering Mechanics, Tsinghua University, Beijing 100084, China)

Received October 21, 2005; revised April 16, 2006

Abstract The flow fields in the blood pump were analyzed three-dimensionally using computational fluid dynamics (CFD). Hemolysis of the pump was calculated based on the changes in shear stress and related exposure times along the particle trace lines using a forward Euler approach. In this way, how different impeller structures and rotational speeds affect the hemolysis was particularly acquired. As a result, impeller with long-short alternant vanes behaved best in hemolysis property and can be utilized to axial blood pumps' development and design.

Keywords: **axial blood pump, computational fluid dynamics, hemolysis.**

Recently, rotary cardiovascular assist devices have been developed and used for recovery of a failing heart or as a bridge to transplantation. As a subset of rotary blood pumps, axial blood pumps have gained tremendous interest as mechanical circulatory support devices due to their small size, favorable anatomical fit, lower power consumption requirements and potential for low cost of manufacturing[1—4]. However, the high rotational speed of axial blood pumps and the small gap between the rotor and housing bring about high shear stresses and hemolysis. Therefore, it is essential to optimize the local flow dynamics inside the axial blood pump to reduce the shear stress, avoid recirculation regions and minimize the residence time of the blood cell inside the pump. As to verification of design modifications *in vitro* hemolysis tests are commonly performed, but the tests require plenty of time and cost.

Recently, computational fluid dynamics (CFD) methods have been widely used as tools for blood pump development and hemolysis analysis of the pumps[5—7]. Hemolysis, the damage of red blood cells, was considered to be function of shear stress and exposure time in previous studies[6,8,9]. In 2001, Apel et al.[5] used the validated computational model of a microaxial blood pump for detailed analysis of shear stress distribution. Several methods are presented that allow for a qualitative assessment of shear stress distribution and related exposure times using a Lagrangian approach and mass distribution in combination with shear stress analysis. In 2003, Mitoh et al.[6] computed the Reynolds shear stress along particle trace lines. Hemolysis was estimated on the basis of shear stress (τ) and its exposure time (t): $dHb/Hb = 3.62 \times 10^{-7} \tau^{2.416} \cdot t^{0.785}$. Particle damage increased with time along the particle trace lines. The computed hemolysis index was in good agreement with the experimental result, which proved that it is possible to explore quantitative function for hemolysis based on shear stress and its exposure time. However, though several experts applied CFD methods to various axial blood pumps[8,9], they simulated simple structures which cannot satisfy the needs for modern axial blood pumps with relative complex structures. In addition, no one tried to utilize CFD methods to find a proper operational speed range for certain axial blood pumps. In this study, we analyzed the flow field of the whole pump including the impeller, flow straightener and diffuser. Hemolysis index of the pump was calculated based on the changes in shear stress and related exposure time along the particle trace lines using a forward Euler approach. The relationship between hemolysis index and rotational speeds was obtained, and by comparing hemolysis index of seven different types of impellers, a new impeller with short-long alternant vanes was proposed, which has the best hemolysis property. This new im-

* Supported by National Natural Science Foundation of China (Grant Nos. 60271006, 60331010)

** To whom correspondence should be addressed. E-mail: deabj@tsinghua.edu.cn

peller structure can be utilized for further development of axial blood pumps.

1 Material and methods

1.1 Axial flow pump

The investigated device is an axial blood pump as shown in Fig. 1. It consists of a pump housing, impeller, flow straightener, and diffuser. The outer diameter of the pump housing was 20 mm, the outer diameter of the impeller was 18 mm, and the hub diameter was 10 mm. The axial gap between the impeller and flow straightener was 1 mm. Seven types of impellers were respectively used in this study, as shown in Fig. 2. The impellers' structures were modified from the original impellers of the DeBakey[1,3] and Jarvik[4]. The numbers of the impellers were chosen to be three to six according to traditional pump designing experiences.

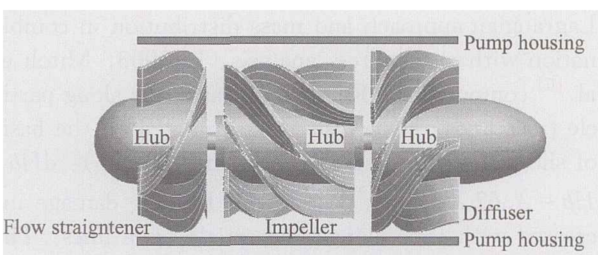

Fig. 1. Structure of the axial blood pump.

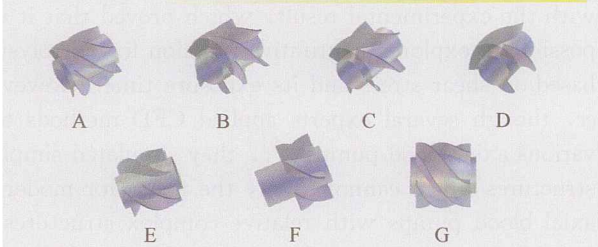

Fig. 2. Structures of seven different impellers.

The impeller is driven by the motor at a maximum speed of 8000 r/min. The maximum pump output is 5 L/min at the physiological pressure levels. Three-dimensional models of the pumps with different impellers were generated on a computer for further fluid dynamic simulation.

The structure of the impeller A in Fig. 2 is the same as the model shown in Fig. 1, models B, C, D have 5, 4, 3 long vanes, respectively. Model E has 3-long and 3-short vanes, model F has 6 short vanes, and the hub of model G is not a cylinder.

1.2 CFD modeling and resolvent

1.2.1 Model and mesh

In this study, the three-dimensional models were divided into hexahedral elements using the grid generation tool (Hexa, oIcemCFD). The entire mesh is J-shaped with an O-grid topology around the vanes. The number of elements is 750000. The computation grids are shown in Fig. 3(a) and Fig. 3(b).

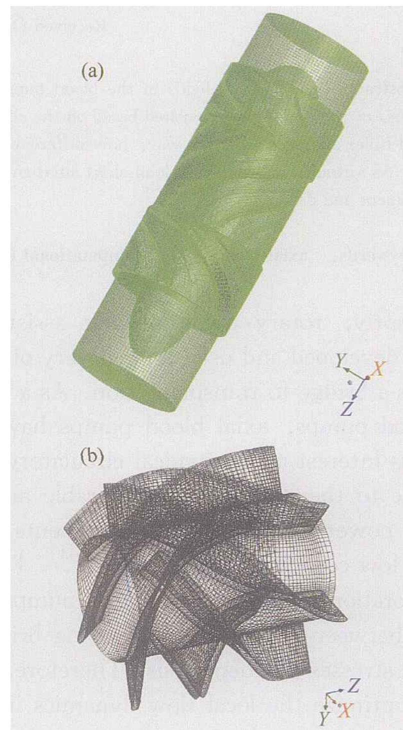

Fig. 3. Computation grids of the axial blood pump. (a) Computation grids of the axial blood pump; (b) Computation grids of the impeller.

1.2.2 CFD analysis

The CFD software package Fluent6.2 was used for boundary setup, post progressing and solving. The inflow was set to be 5 L/min and the outlet pressure was set to be 1.01×10^5 Pa at the outlet of the pump housing. A low turbulent intensity of 0.01 was set at the inflow boundary. The wall was defined as a non-slip wall. The impeller region was defined as a rotating frame and the stage-rotor and transient-rotor computations were applied for the calculations of macroscopical fluid parameters and details of the whole flow field, respectively.

Blood was assumed to be an incompressible Newtonian fluid with a density of 1059 kg/m^3 and a constant viscosity of 3.6×10^{-3} Pa·s.

Small-scale turbulence is not expected to play a significant role in force generation. Therefore, for simplicity, a two-equation Reynolds averaged Navier-Stokes turbulence model[11] has been used rather than transient specific models, such as large eddy simulation or detached-eddy simulation (DES). The point of flow separation is important to predict the shear and pressure forces acting on vanes, but the traditional *k-e* turbulence model cannot accurately predict the separation point. Therefore, the shear stress transport (SST) turbulence model is used to better indicate flow separation. When the node resolution of the near wall region is sufficiently high, the *k-w* model makes a more accurate description of the near wall region. In regions with low grid density, the implemented *k-w* model automatically switches back to the conventional wall function.

1.3 Calculation of hemolysis estimation

Mechanism of blood damage and effects of shear stress on blood corpuscles were investigated by Giersiepen et al.[10]. The following basic model for estimation of blood damage is proposed as

$$dHb/Hb = 3.62 \times 10^{-7} \cdot \tau^{2.416} \cdot t^{0.785}, \quad (1)$$

where Hb is the hemoglobin concentration, dHb is the increase in the plasma free hemoglobin concentration, τ is the shear stress, and t is the exposure time.

The quantity $-\rho\,\overline{u_i u_j}$ is known as the Reynold stress tensor and is a symmetric tensor:

$$\rho\,\overline{u_i u_j} = \begin{bmatrix} \rho\overline{u}^2 & \rho\,\overline{uv} & \rho\,\overline{uw} \\ \rho\,\overline{vu} & \rho\overline{v}^2 & \rho\,\overline{vw} \\ \rho\,\overline{wu} & \rho\,\overline{wv} & \rho\overline{w}^2 \end{bmatrix}, \quad (2)$$

where u, v, w are the fluctuating components of the fluid mean velocity along x-axis, y-axis and z-axis. Fluent 6.2 provides these values at each node.

The viscous stress σ_{ij} is a nine-component tensor. As a Newtonian fluid, the viscous stress of the blood is proportional to the element strain rates and the coefficient of viscosity μ:

$$\sigma_{ij} = \mu\left(\frac{\partial u_i}{\partial x_j} + \frac{\partial u_j}{\partial x_i}\right). \quad (3)$$

The shear stress in the turbulent flow was obtained as a summation of the viscous and Reynolds shear stress:

$$\tau_{ij} = \sigma_{ij} + \rho\,\overline{u_i u_j}. \quad (4)$$

With the method proposed by Bludsuweit[10], the shear stress value at each node was given as:

$$\tau = \left[\frac{1}{6}\sum(\tau_{ii} - \tau_{jj})^2 + \sum\tau_{ij}^2\right]^{\frac{1}{2}}. \quad (5)$$

Through the particle tracking command of Fluid 6.2, the particle lines were obtained by using a forward Euler approach:

$$x_i^t = x_i^{t-1} + v_i\Delta t, \quad (6)$$

where x_i^{t-1} and x_i^t are locations of particle at the preceding and present time step, Δt is the time interval, and v_i is the local speed vector of fluid element i. It is assumed that the effect of shear stress on red cells can be summed along the particle trace.

For each red blood cell, the increase in the rate of damage for a time interval is expressed as:

$$d_{p,i} = 3.62 \times 10^{-7} \times \tau(t = t_{i-1})^{2.416} \times (t_i - t_{i-1})^{0.785}, \quad (7)$$

where p indicates the number of the trace lines. The initial damage D_0 was set to be zero, and the accumulated damage D_p for the p-th particle trace line from time zero to t_i was expressed as:

$$D_{p,i} = D_{p,i-1} + (1 - D_{p,i-1})d_{p,i}. \quad (8)$$

For all the particle trace lines, the damage of the red blood cells could be calculated. The estimated hemolysis index E was defined as the average damage of all the trace lines:

$$E = \frac{1}{N}\sum_{P}^{N} D_P. \quad (9)$$

If enough particle trace lines are taken into account, estimation errors of E can be neglected.

2 Simulation results

2.1 Distribution of shear stress

Fig. 4 shows the distribution of shear stress on the axial section, and Fig. 5 shows the distribution of shear stress along the particle trace lines. In the above two figures, high shear stress is observed mainly in the region near the interface between the rotating impellers and diffusers, and the gap between the edges of the impellers and housing has shear stress over 1000 Pa. Therefore, better structures of impellers and diffusers should be proposed to decrease shear stress.

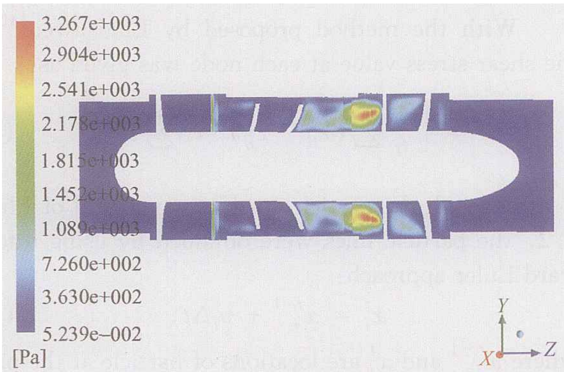

Fig. 4. Distribution of shear stress on the axial section.

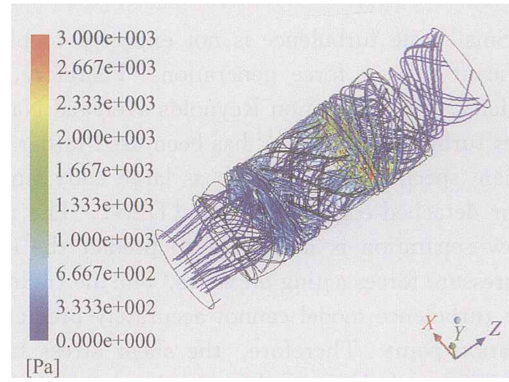

Fig. 5. Distribution of shear stress along the particle trace lines.

2.2 Estimation of hemolysis

The hemolysis index E modified with different numbers of particle trace lines, and its error can be neglected when over 100 particles are taken into account, as shown in Table 1.

Table 1. Hemolysis index E with different numbers of particles

Numbers	345	296	258	230	207	104	70	52	42	35	30	14	8
E	0.031	0.030	0.030	0.031	0.031	0.031	0.029	0.033	0.028	0.031	0.026	0.025	0.035

Fig. 6 shows the estimated hemolysis damage when the axial blood pump operated at different rotational speeds ranges from 3000 r/min to 8000 r/min. With the increasing rotational speeds, the hemolysis of the blood cell increases obviously. Relative hemolysis index E_{REL} is equal to E/E_{8000}, where E_{8000} is hemolysis index of pump with impellers as model A in Fig. 2 when it is operated at 8000 r/min.

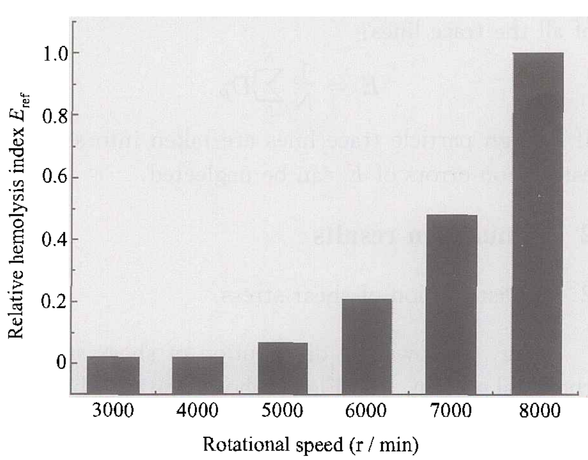

Fig. 6. Relationship between rotational speed and relative hemolysis index.

Fig. 7 shows the estimated hemolysis results of pumps with different types of impellers at 8000 r/min, and the 6-long vane's relative hemolysis index is the highest. The hemolysis index of the pump with the 3-long vane was the lowest, with the 4-long vane impeller and the 3-long 3-short vane impeller followed. Among all the 6-vane structures, model E behaves best in the hemolysis property. This new impeller design should be applied to the development of axial blood pumps.

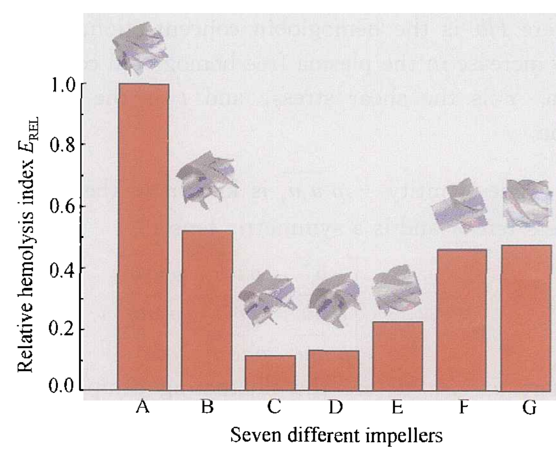

Fig. 7. Relative hemolysis index of pumps with seven different impellers.

3 Discussion and conclusions

This study introduced CFD methods to estimate the hemolysis property and fluid dynamic parameters of axial blood pumps which otherwise cannot be obtained in detail from *in vivo* experiments. For accuracy of CFD simulations and calculations, appropriate turbulence and near wall model were applied. Stage-rotor computation was accurate enough for macroscopical fluid parameters, such as the pump's pressure head, efficiency and hemolysis analysis. However, transient-rotor computation had to be taken into account for details of the whole flow field. To predict the shear and pressure forces, the shear stress transport (SST) turbulence model is used to better explain flow separation.

According to the results of CFD analysis, high shear stress can be observed mainly in the region between the rotating impellers and diffusers and the gap between the edges of the impellers and housing. Because diffusers are used to translate the rotational flow to the axial flow to increase pressure head, proper discharge angle and generatrix should be utilized to avoid high shear stress in the region between the impellers and diffusers.

In this study, hemolysis of the pump is calculated based on the changes in shear stress and related exposure times along the particle trace lines using a forward Euler approach. Only when at least 100 particles are included, can the error of hemolysis index be neglected. The hemolysis index of the blood cell in the pump strongly depends on the numbers and structure of the impellers. The impeller with long-short alternant vanes behaves better than those with all long or all short vanes in hemolysis property.

In addition, the rotational speed is another important factor influencing the hemolysis of the blood cell. According to Fig. 6, when the rotational speed increases in the range of from 3000 r/min to 5000 r/min, hemolysis index increases slowly. However, above 6000 r/min, the pump's hemolysis index increases rapidly. In conclusion, there is a conic relationship between the rotational speed and hemolysis index.

In sum, according to the above calculation and fluid simulation of axial blood pumps with seven different impellers operating at six different constant speeds ranging from 3000 r/min to 8000 r/min, a preferred impeller structure with the best hemolysis property is attained: the 3-long 3-short vane impeller. And the preferred operating constant speed is 6000 r/min, which is the turning point above which the pump's hemolysis index increases sharply.

References

1 DeBakey M. E. Development of a ventricular assist device. Artif Organs, 1997, 21: 1149—1153.

2 Butler K.C., Maher T.R. and Borovetz H.S. Development of an axial flow blood pump. ASAIO J., 1992, 38: 296—300.

3 Debakey M. E. The odyssey of the artifical heart. Artif Organs, 2000, 24: 405—411.

4 Frazier O.H., Myers T.J., Jarvik R.K. et al. Research and development of an implantable, axial-flow left ventricular assist device: the Jarvik 2000 Heart. Ann. Thoracic. Surg., 2001, 71: S125—132.

5 Apel J., Paul R., Klaus S. et al. Assessment of hemolysis related quantities in a microaxial blood pump by computation fluid dynamic. Artif Organs, 2001, 25: 341—347.

6 Mitoh A., Yano T., Sekine K. et al. Computational fluid dynamics analysis of an intra-cardiac axial flow pump. Artif Organs, 2003, 27: 34—40.

7 Yano T., Sekine K., Mitoh A. et al. An estimation method of hemolysis within an axial flow blood pump by computational fluid dynamic analysis. Artif Organs, 2003, 27: 920—925.

8 Bludszuweit C. A theoretical approach of the prediction of hemolysis in centrifugal pumps. PhD Thesis, University of Strathclyde, Glasgow, 1994.

9 Yeleswarapu K.K., Antaki J.F., Kameneva M.V. et al. A mathematical model for shear-induced hemolysis. Artif Organs, 1995, 19: 576—582.

10 Giersiepen M., Wurzinger L.J., Opitz R. et al. Estimation of shear stress-related blood damage in heart valve prostheses *in vitro* comparison of 25 aortic valves. Int. J. Artif. Organs, 1990, 13: 300—306.

11 Launder B. E. and Spalding D. B. Lectures in Mathematical Models of Turbulence. London: Academic Press, 1972.